



HAL
open science

Dual-band dual-linearly polarized transmitarray at Ka-band

Reda Madi, Antonio Clemente, Ronan Sauleau

► **To cite this version:**

Reda Madi, Antonio Clemente, Ronan Sauleau. Dual-band dual-linearly polarized transmitarray at Ka-band. EuMW 2020 - European Microwave Week 2020, Jan 2021, Utrecht, Netherlands. 10.23919/EuMC48046.2021.9337962 . cea-03637082v2

HAL Id: cea-03637082

<https://cea.hal.science/cea-03637082v2>

Submitted on 11 Apr 2022

HAL is a multi-disciplinary open access archive for the deposit and dissemination of scientific research documents, whether they are published or not. The documents may come from teaching and research institutions in France or abroad, or from public or private research centers.

L'archive ouverte pluridisciplinaire **HAL**, est destinée au dépôt et à la diffusion de documents scientifiques de niveau recherche, publiés ou non, émanant des établissements d'enseignement et de recherche français ou étrangers, des laboratoires publics ou privés.

Dual-Band Dual-Linearly Polarized Transmitarray at Ka-Band

Reda Madi^{#1}, Antonio Clemente^{#2}, Ronan Sauleau^{*3}

[#]CEA-Leti, MINATEC Campus, F-38054 Grenoble, France

⁺Univ. Grenoble-Alpes, 38400 Grenoble, France

^{*}Univ Rennes, CNRS, IETR, UMR 6164, F-35000 Rennes, France

{¹reda.madi, ²antonio.clemente}@cea.fr, ³ronan.sauleau@univ-rennes1.fr

Abstract — We present here the design and the optimization of a dual-band dual linearly-polarized transmitarray antenna with a 1-bit phase resolution (*i.e.* two phase states with 180° of relative phase-shift). The antenna operates in both downlink and uplink K/Ka-bands (17 – 21 GHz for the lower frequency band, and 27 – 31 GHz for the upper one) and could be used for satellite communication applications. In order to implement dual-band and dual-polarization, the unit-cell consists of four orthogonal superposed U-slotted patch antennas interconnected by a metallized via hole. A 20×20 transmitarray based on the proposed unit-cell architecture has been optimized by using our *in-house* tool and validated through full-wave electromagnetic simulations. The 5×5 mm² unit-cell size allows beam scanning over large field of view (up to 80°). A maximum gain of 23.4 and 21.4 dBi has been achieved at 29.1 GHz and 19.5 GHz, respectively. The gain 1-dB bandwidth is equal to 17.4% and 10.5% at the lower and the upper frequency bands, respectively.

Keywords — Transmitarray antenna, SATCOM, dual-band, dual-polarization, dual-linear polarization.

I. INTRODUCTION

During the last decade, transmitarray antennas, also referred in the literature as discrete lenses, have been extensively studied and investigated due to their promising properties in terms of compactness, low cost, lightweight, and high gain performance [1]. Their spatial feeding mechanism allows to reduce the insertion loss of the power division network if compared to classical arrays, and is compatible with the implementation of low-profile transmitarrays [2], [3]. Furthermore, Printed Circuit Board (PCB) technologies allows the integration of solid state components on the radiating panel enabling the possibility to implement electronically beam-scanning and beam-forming [4].

Specifications for Satcom-on-the-move (SOTM) applications require two independent steerable antenna systems for both uplink and downlink. For such applications the proposed transmitarray antenna is believed as a good candidate, considering its dual-band and dual-polarization properties. So far only a few fixed beam transmitarrays propose dual-band operating at K/Ka-band [6]-[10]. Electronically steerable transmitarrays operating in linear or switchable-circular polarization have been successfully demonstrated at Ka-band in our previous work [4]. The possibility to implement a dual

linearly-polarized steerable transmitarray has also been presented in our preliminary work [5].

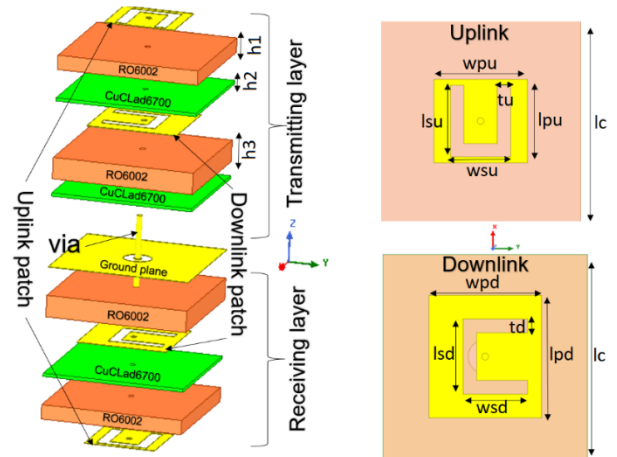


Fig. 1. 3-D exploded view of the proposed 1-bit K/Ka-band unit-cell.

In this paper, we propose a structure that can achieve a very large field of view, up to 80° , independently in both bands. Indeed stacking the resonant elements, instead of interleaving them [6]-[10], allows us to have a unit-cell electrical size that is smaller than half the wavelength in the uplink and downlink.

This paper is organized as follows. Section II explains the design principle for the transmitarray antenna, describing the unit-cell with the simulation results. Then, the full-wave simulation results are provided in section III. Finally, conclusion and perspectives are discussed in section IV.

Table 1. Dimensions of the parameters of the unit-cell for the uplink and downlink element.

Parameters (uplink)	Value (mm)	Parameters (downlink)	Value (mm)
L_c	5	L_c	5
h_1	0.508	h_1	0.508
h_2	0.014	h_2	0.014
h_3	0.762	h_3	0.762
W_{pu}	2.50	w_{pd}	3.20
L_{su}	2.10	l_{sd}	1.96
W_{su}	1.80	w_{sd}	1.93
L_{pu}	2.50	l_{pd}	3.20
t_u	0.40	t_d	0.38

II. DESIGN AND OPTIMIZATION OF THE DUAL-BAND DUAL-POLARIZED UNIT-CELL

A. Superposition principle

The proposed dual-band, dual-polarized transmitarray antenna is based on a linearly-polarized unit-cell with orthogonal polarization. It consists of four U-slotted patch antennas, operating at 19 GHz for the lower frequency band and at 29 GHz for the upper one (downlink and uplink, respectively). They are stacked on different layers and connected with a metallic via, as shown in Fig. 1. To the best of our knowledge this superposition technique for dual band operation has never been studied for transmitarrays.

B. Unit-cell design

The studied unit-cell architecture is represented in Fig. 1. Its overall size equals 5×5 mm², equivalent to $0.48\lambda_{ul} \times 0.48\lambda_{ul}$ and $0.32\lambda_{dl} \times 0.38\lambda_{dl}$, where λ_{ul} and λ_{dl} stand for the free space wavelength at 29 and 19 GHz, respectively. Such a small lattice size allows us to scan the antenna beam over a wide field of view, both in the downlink and uplink bands.

More precisely, four U-shaped slot loaded patch antennas are used in this design, two patches for the receiving layer and two patches for the transmitting one. The inner metal layers (patches resonating at the lower frequency and ground plane) are printed on two 0.762-mm-thick substrates (Roger RT/Duroid 6002 substrates $\epsilon_r = 2.94$, $\tan\delta = 0.0012$) and are linearly-polarized along y -axis. The outer metal layers (corresponding to patches resonating at the higher frequency) are printed on two 0.508-mm-thick substrates and are polarized along x -axis. These substrates are bounded using a thin film (Arlon CuClad 6700 films $\epsilon_r = 2.35$, $\tan\delta = 0.0025$). These four patches are connected by a metallic via, with a metallic ground plane placed between the receiving and the transmitting layers in order to isolate these two parts.

With this configuration, we can achieve a 1-bit of phase resolution in both bands independently, by rotating the transmitting patches (or the receiving patches) by 180° around the central metallized via. Rotating the patch resonating at the higher frequency leads to a 180° phase shift for the uplink, and rotating the patch resonating at the lower frequency gives us 180° phase shift for the downlink. The two unit-cell phase states are called UC0 and UC180, respectively.

C. Simulation results

The proposed unit-cell has been simulated using the full-wave electromagnetic software Ansys HFSS (v.18.2) with periodic boundary conditions and Floquet ports. Dielectric and ohmic losses are taken into account in the simulations. The magnitude of the simulated scattering parameters is depicted in Fig. 2. Note that only normal incidence is considered here.

The 1-dB transmission bandwidth of the proposed unit-cell reaches 17.4% and 10.5% at 19.5 GHz and 29 GHz respectively with an insertion loss lower than 0.5 dB. We can also see in Fig. 3, the transmission phase of the unit-cell showing that 180° phase shift is achieved (1-bit of phase resolution) over the entire band of interest, in the lower and higher frequency.

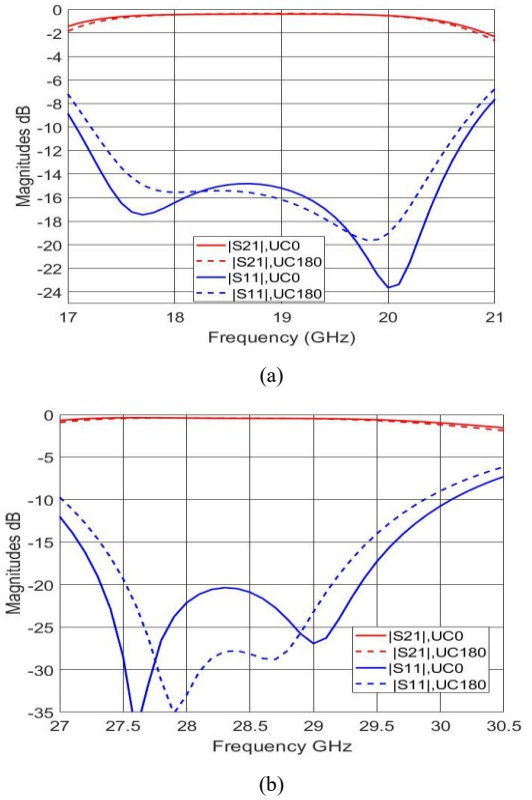


Fig. 2. Magnitude of the transmission and reflection coefficients of the unit-cell in (a) downlink band and (b) uplink band for both phase state.

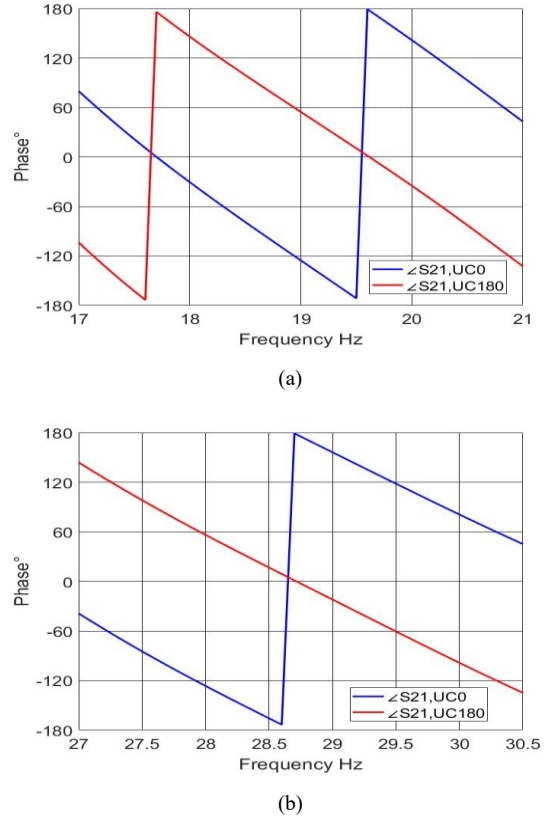


Fig. 3. Transmission phase of the unit-cell in (a) downlink band and (b) uplink band for both phase state.

III. DUAL-BAND DUAL-POLARIZED TRANSMITARRAY

The 1-bit unit-cell presented in Section II is used to implement a high-gain transmitarray. It consists of two stacked square arrays of 20×20 elements (the outer array is used for the uplink while the inner one is for the downlink). The radiation characteristics of the transmitarray are computed using our *in-house* CAD simulation tool, based on an analytical model of the array and full-wave simulations of the focal source and the unit-cells. These theoretical results are validated here through full-wave electromagnetic simulations (Ansys HFSS). To illuminate the array, two pyramidal horns are used: ATM 34-440-6 for the uplink (11.4-dBi gain) and ATM 51-440-6 (11.2-dBi gain) for the downlink. The two horns are located in the same focal plane at a distance $F = 60$ mm from the array aperture ($F/D = 0.6$) with an offset of ± 13 mm along the y -axes. They are orthogonally polarized, x -polarized for the uplink horn and y -polarized for the downlink. The Fig. 4 shows the dual-band transmitarray with offset horns, note that (a) and (b) represent the same transmitarray, for clearance purposes the outer layer is hidden in (b) to see the downlink phase distribution. The focal distance and the phase distributions have been optimized to maximize the transmitarray gain and the aperture efficiency independently on each frequency bands.

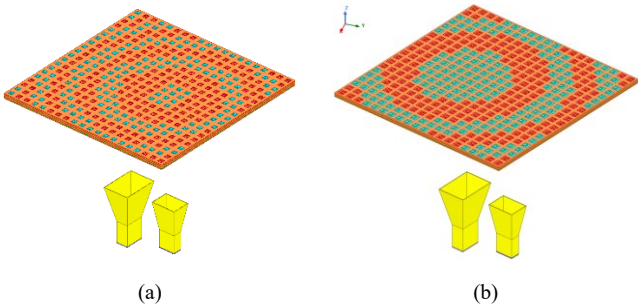


Fig. 4. Dual-band transmitarray showing two independent phase distribution, (a) for the uplink and (b) for the downlink.

The main challenge of this design is to calculate the 1-bit phase distributions on both frequency bands, downlink (DL) and uplink (UL), required to independently steer the beams in a specific direction. The computed distributions optimized to collimate the beams at broadside for the two bands are plotted in Fig. 5(a) and Fig. 5(b), respectively. Its combination into the same layout gives us the unit-cell distribution presented in Fig. 5(c). Here, the states 0DL-0UL and 0DL-180UL indicate the combination of a unit-cell 0° in the downlink with a unit-cell 0° or 180° in the uplink. Contrariwise, the states 180DL-0UL and 180DL-180UL indicate the combination of a unit-cell 180° in the downlink with a unit-cell 0° or 180° in the uplink. It is important to notice, that these four unit-cell combinations have been considered during the optimization process of the transmitarray with the *in-house* tool to take into account the coupling between the two bands and polarizations.

The broadside gain computed in both bands as a function of the frequency is represented in Fig. 6. Here, the results achieved with the *in-house* tool are compared to the full-wave electromagnetic simulations. An acceptable agreement can be observed with an average error < 1 dB. A maximum gain of

23.4 and 21.4 dBi has been achieved at 29.1 and 19.75 GHz, respectively.

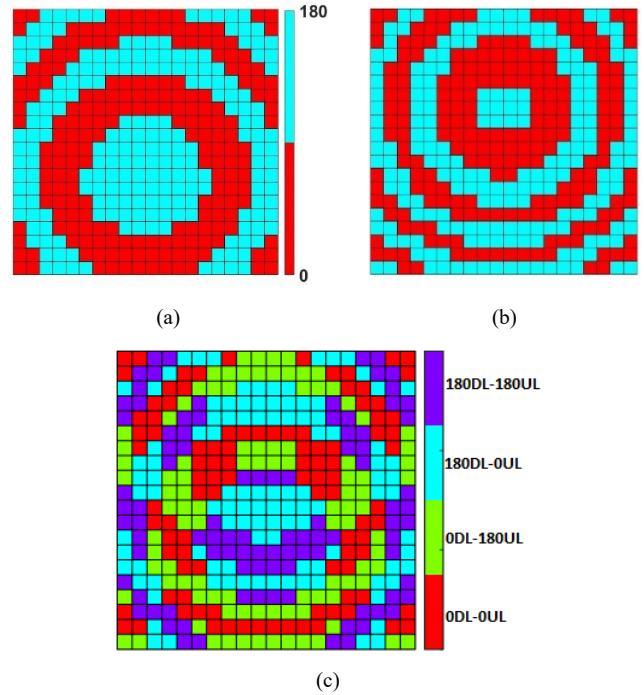


Fig. 5. Phase distribution layout for broadside radiation: (a) downlink, (b) uplink and (c) final combined layout.

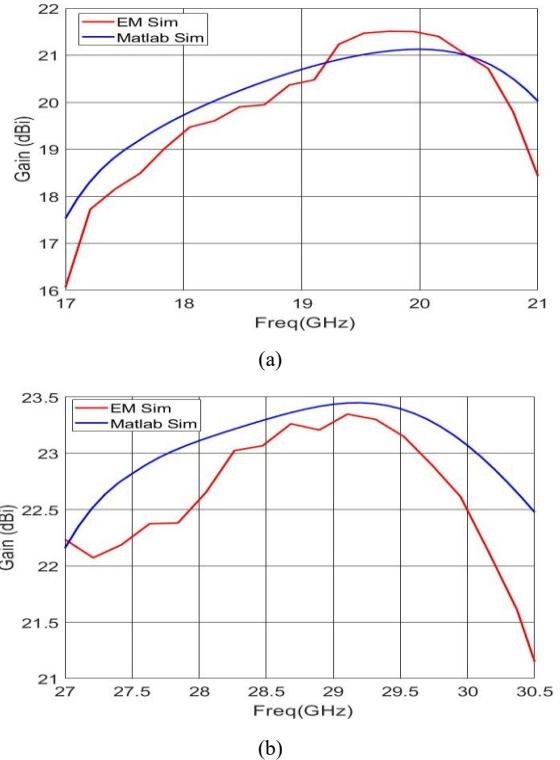


Fig. 6. Simulated gain for the downlink (a) and for the uplink (b).

The radiation patterns computed on the E-plane at broadside for the frequencies 19 and 29 GHz are represented in Fig. 7, respectively. The side lobe level remains around 16.4 dB below

the maximum for both bands at both frequencies. Also in this case, an acceptable agreement has been achieved between the results obtained with our *in-house* tool and full-wave electromagnetic simulations. The obtained results are synthesized and compared to the current state of the art on dual-band dual-polarized transmitarray in Table 2.

To discuss the impact of the coupling between the two frequency bands two simulations have been done. In the first one (TA-I), the radiated beam at the uplink is steered with an angle of -40° on the E-plane when the downlink beam it is collimated at broadside. In the second simulation (TA-II), the radiated beam remains the same in the uplink and the downlink radiated beam is steered at 50° on the H-plane. The Fig. 8 shows that the impact on the co-polar component is negligible.

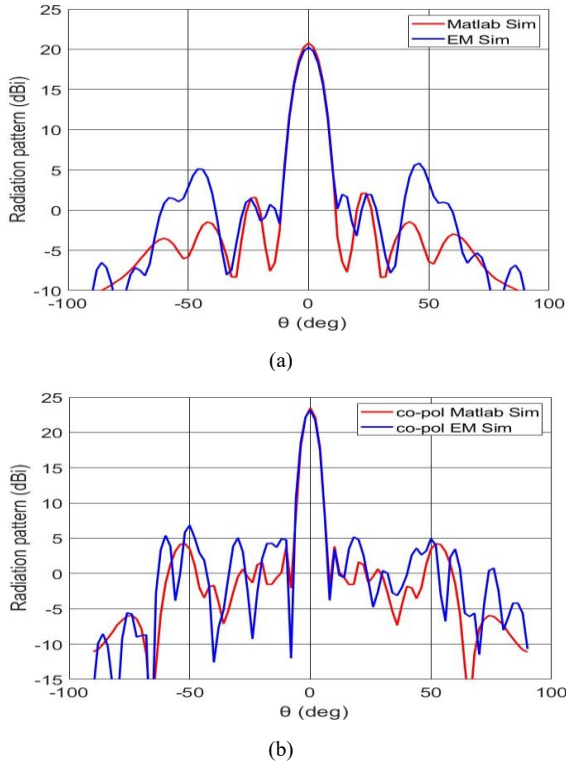


Fig. 7. Simulated radiation pattern for both bands (a) downlink and (b) uplink

Table 2. Comparison of the proposed TA with the state of the art on dual-band transmitarray.

Ref	Freq (GHz)	Pol.	3-dB BW (%)	Gain (dBi)	F/D	AE (%)
[6]	20.0 30.0	Dual LP	11.3 11.4	27.0 28.4	0.6	20.1 21.2
[7]	20 30	Single CP	10 7	15.3 15.3	0.69	10 6
[8]	11 12.5	Dual LP	6.8 5.4	23.6 24.4	0.8	38 34.6
[9]	12 18	Single LP	3.3 3.4	27.8 31.4	0.8	52 53
[10]	12.0 14.2	Dual CP	7.5 7.0	23.9 24.5	0.65	32.2 28.9
This work	19.8 29.1	Dual LP	> 19.8 > 12.0	21.4 23.4	0.6	25.1 20.0

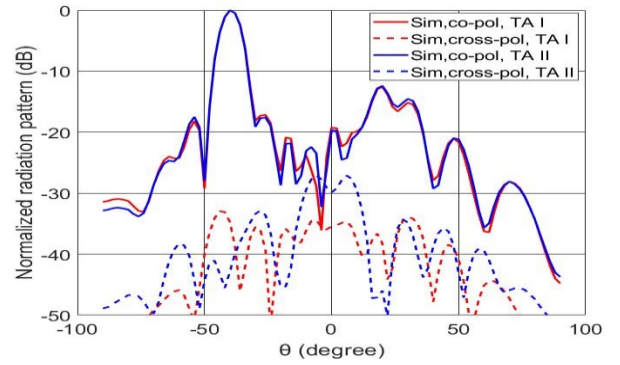


Fig. 8. Simulated normalized radiation patterns in E-plane at 29 GHz for TA-I and TA-II.

IV. CONCLUSION

A dual-band dual-polarized unit-cell based on the superposition technique is presented. It consists of four U-slotted patches stacked on different layers. The phase control is obtained by rotating the transmitting layer (a rotation of 180 degrees), achieving 1-bit of phase quantization.

A 20×20 -element transmitarray antenna is simulated using the proposed unit-cell. It exhibits a maximum gain of 23.4 and 21.4 dBi with an aperture efficiency of 18.7% and 23.7% at 29.1 GHz and 19.75 GHz, respectively. For future perspectives, the same concept can be used for circular polarization and by adding active elements we could provide reconfigurability.

REFERENCES

- [1] S. V. Hum and J. Perruisseau-Carrier, "Reconfigurable reflectarrays and array lenses for dynamic antenna beam control: A review," *IEEE Trans. Antennas Propag.*, vol. 62, no. 1, pp. 183–198, Jan. 2014.
- [2] G. Nicholls and S. V. Hum, "Full-space electronic beam-steering transmitarray with integrated leaky-wave feed," *IEEE Trans. Antennas Propag.*, vol. 64, no. 8, pp. 3410–3422, Aug. 2016.
- [3] A. Clemente, M. Smerchalski, M. Huchard, T. Le Nadan, and C. Barbier, "Characterization of a low-profile quad-feed based transmitarray antenna at V-band," in *Proc. 49th European Microw. Conf. (EuMC 2019)*, Paris, France, 2019.
- [4] A. Clemente, L. Di Palma, F. Diaby, L. Dussopt, K. Pham, and R. Sauleau, "Electronically-steerable transmitarray antennas for Ka-Band," in *Proc. 13th Eur. Conf. Antennas Propag. (EuCAP 2019)*, Krakow, Poland, Mar. 2019.
- [5] K. Pham, R. Sauleau, A. Clemente, and L. Dussopt, "Electronically reconfigurable unit-cell and transmitarray in dual-linear polarization at Ka-band," *13th Europ. Conf. Antennas Propag. (EuCAP 2019)*, Krakow, Poland, Mar. 2019.
- [6] K. T. Pham, R. Sauleau, E. Fourn, F. Diaby, A. Clemente, and L. Dussopt, "Dual-Band transmitarrays with dual-linear polarization at Ka-band," *IEEE Trans. Antennas Propag.*, vol. 65, no. 12, pp. 7009–7018, 2017.
- [7] H. Hasani, J. S. Silva, S. Capdevila, M. Garcia-Viguera, and J. R. Mosig, "Dual-band circularly polarized transmitarray antenna for satellite communications at 20/30 GHz," *IEEE Trans. Antennas Propag.*, vol. 67, no. 8, pp. 5325–5333, 2019.
- [8] M. O. Bagheri, H. R. Hassani, and B. Rahmati, "Dual-band, dual-polarised metallic slot transmitarray antenna," *IET Microw. Antennas and Propag.*, vol. 11, no. 3, pp. 402–409, 2017.
- [9] R. Y. Wu, Y. B. Li, W. Wu, C. B. Shi, and T. J. Cui, "High-gain dual-band transmitarray," *IEEE Trans. Antennas Propag.*, vol. 65, no. 7, pp. 3481–3488, 2017.
- [10] Y. M. Cai, K. Li, W. Li, S. Gao, Y. Yin, L. Zhao, and W. Hu, "Dual-band circularly polarized transmitarray with single linearly polarized feed," *IEEE Trans. Antennas Propag.*, in press.